Solar Phys (2008) 253: 215–235
DOI 10.1007/s11207-008-9241-5

Origin of Coronal Shock Waves

Invited Review

Bojan Vršnak · Edward W. Cliver

Received: 29 November 2007 / Accepted: 24 June 2008 / Published online: 29 July 2008

Abstract The basic idea of the paper is to present transparently and confront two different views on the origin of large-scale coronal shock waves, one favoring coronal mass ejections (CMEs), and the other one preferring flares. For this purpose, we first review the empirical aspects of the relationship between CMEs, flares, and shocks (as manifested by radio type II bursts and Moreton waves). Then, various physical mechanisms capable of launching MHD shocks are presented. In particular, we describe the shock wave formation caused by a three-dimensional piston, driven either by the CME expansion or by a flare-associated pressure pulse. Bearing in mind this theoretical framework, the observational characteristics of CMEs and flares are revisited to specify advantages and drawbacks of the two shock formation scenarios. Finally, we emphasize the need to document clear examples of flare-ignited large-scale waves to give insight on the relative importance of flare and CME generation mechanisms for type II bursts/Moreton waves.

Keywords Shock waves · Magnetohydrodynamics (MHD) · Sun: corona · Sun: coronal mass ejections (CMEs) · Sun: flares

1. Introduction

Solar flares and coronal mass ejections (CMEs) are explosive phenomena in the solar atmosphere, viable of launching global large-amplitude coronal disturbances and shock waves. The longest-known signatures of coronal shock waves are radio type II bursts (Payne-Scott, Yabsley, and Bolton, 1947; Wild and McCready, 1950) and Moreton waves (Moreton,

Radio Physics and the Flare-CME Relationship
Guest Editors: Karl-Ludwig Klein and Silja Pohjolainen.

B. Vršnak (✉)
Faculty of Geodesy, Hvar Observatory, Zagreb, Croatia
e-mail: bvrsnak@geof.hr

E.W. Cliver
Research Vehicles Directorate, Air Force Research Laboratory, Hanscom AFB, MA 01731-3010, USA

1960; Moreton and Ramsey, 1960). The type II burst is a narrow-band radio emission excited at the local plasma frequency (and/or harmonic) by a fast-mode MHD shock (*e.g.*, Nelson and Melrose, 1985, and references therein). As the shock propagates outwards through the corona, the emission drifts "slowly" (in comparison with fast-drift type III emission) towards lower frequencies due to decreasing ambient density. Radial velocities, inferred from the emission drift rates by using various coronal density models, are found to be in the order of 1000 km s^{-1}. The Moreton wave is a large-scale wave-like disturbance of the chromosphere, observed in Hα, which propagates out of the flare site at velocities also in the order of 1000 km s^{-1}. In this respect it is worth noting that first indications of global coronal disturbances were provided by flare-associated activations of distant filaments (Dodson, 1949; see also Ramsey and Smith, 1966).

The MHD model unifying both phenomena in terms of the fast-mode shock wave was proposed by Uchida (1974). According to Uchida's (1968) "sweeping-skirt" scenario, the Moreton wave is the surface track of the fast-mode MHD coronal shock propagating out of the source region along "valleys" of low Alfvén velocity, *i.e.*, being refracted from the high Alfvén velocity regions and enhanced in low velocity regions. At larger heights, the shock causes the type II burst.

More recently, an EUV counterpart of the Moreton wave was reported by Neupert (1989), and a decade later these coronal disturbances were directly imaged by the Extreme-ultraviolet Imaging Telescope (EIT; Delaboudinière *et al.*, 1995) on the Solar and Heliospheric Observatory (SoHO). The discovery of "EIT-waves" (Moses *et al.*, 1997; Thompson *et al.*, 1998) prompted a search for wave signatures in other spectral domains. Soon, the Moreton-wave associated disturbances were revealed in soft X-rays (Narukage *et al.*, 2002; Khan and Aurass, 2002; Hudson *et al.*, 2003; Warmuth, Mann, and Aurass, 2005), He I 10 830 Å (Gilbert *et al.*, 2001; Vršnak *et al.*, 2002a; Gilbert and Holzer, 2004), and microwaves (Warmuth *et al.*, 2004a; White and Thompson, 2005); for an overview and historical background see, *e.g.*, Cliver *et al.* (2004) and Zhukov and Auchère (2004). Warmuth *et al.* (2004a, 2004b) investigated the morphology and kinematics of 12 large-scale wave events and argued for a common origin of propagating disturbances seen in the various spectral channels.

It is important to note that some of propagating EUV signatures denoted as "EIT-waves" are probably not a wave phenomenon, but rather a consequence of some other processes related to the large scale magnetic field reconfiguration. EIT disturbances of this kind are usually much slower and more diffuse than those representing the coronal counterpart of the Moreton waves (Warmuth *et al.*, 2004a, 2004b) and those accompanied by type II bursts (Biesecker *et al.*, 2002). Such non-wave events either could be a consequence of the CME associated field-line "opening" (*e.g.*, Chen *et al.*, 2005), or could be caused by various forms of coronal restructuring driven by the eruption (*e.g.*, Delannée and Aulanier, 1999; Attrill *et al.*, 2007). In the following we do not consider such non-wave phenomena, *i.e.*, we focus only on true large-scale coronal MHD waves.

2. Flare *vs*. CME Controversy: Defining the Problem

Generally, large-amplitude MHD waves in the corona are tightly associated with CMEs and flares. The source of the coronal wave seems clear in events where the CME is accompanied only by a very weak/gradual flare-like energy release. In such cases the type II bursts characteristically start in the frequency range well below 100 MHz (Shanmugaraju *et al.*, 2008). The situation is different for Moreton-wave associated type II bursts, which tend to have considerably higher starting frequencies, with emission in the harmonic band occasionally extending to > 300 MHz range (Warmuth *et al.*, 2004b; Vršnak *et al.*, 2006). In such events both the CME and the flare are observed, so over the years a flare *vs*. fast ejection controversy has arisen regarding the origin of coronal shocks (Cliver, Webb, and Howard, 1999; Vršnak, 2001; Hudson *et al.*, 2003; Hudson and Warmuth, 2004; Cho *et al.*, 2005; Shanmugaraju *et al.*, 2005; Gopalswamy, 2006; Pohjolainen and Lehtinen, 2006; Reiner *et al.*, 2007; Magdalenić *et al.*, 2008).

More specifically, the shock could be driven over large distances by the eruption of a structure that evolves to a CME, or can be ignited by a smaller scale process associated with the flare energy release, *e.g.*, expansion of hot loops or small-scale ejections. In this respect, it is important to make a clear distinction between the shock driver and the shock formation mechanism. The basic mechanism of the wave formation could be similar even if the driver has an entirely different physical nature. For example, the magnetically driven CME and an expansion of hot flare loops caused by a pressure pulse would both form the wave by the three-dimensional (3D) piston mechanism (see Chapter 4 in Sedov, 1959). The difference appears only in the later evolution of the wave, since in the former case the wave is permanently supplied by the energy from the CME, whereas in the latter case it behaves as freely propagating large-amplitude wave. On the other hand, motions that are predominantly one-dimensional, *e.g.*, plasma blobs, would cause a shock (for a possible example see Klein *et al.*, 1999) in a manner similar to moving projectiles of constant size (for details see Chapter XIII in Landau and Lifshitz, 1987).

Thus, we first have to define two basic processes of the shock formation. In the case of a "projectile mechanism", the plasma is pushed forward ahead of the driver, whereas behind and aside of the driver it moves in a complex manner, since the space behind the driver has to be filled-up by the plasma and there is a flow associated with the sidewise propagation of the shock flanks. Since the driver propagates *through* the ambient medium, we say that the plasma flows past the driving body. In the situation when the driver has constant size (rigid body), it must be supersonic to produce the shock. This type of shock is called a bow-shock. In a homogeneous ambient medium the offset distance between the bow-shock and the driver is constant (*i.e.*, the velocities of the driver and the shock are equal) and depends on the driver velocity (Mach number), as well as on the size and the shape of the driver (Russell and Mulligan, 2002). In the case of a blunt driver, the shock-front forms approximately a hyperbolic surface whose distant flanks asymptotically attain the form of the Mach cone (see Chapters IX and XIII in Landau and Lifshitz, 1987).

In the case of a 3D piston, the expanding driver pushes the plasma in all directions as in, *e.g.*, a supernova explosion. The one-dimensional analog is a piston in a tube, where the gas ahead of the piston cannot be transposed to behind the piston. In such a case the shock can be formed even if the piston is "subsonic" (*e.g.*, see Problem 1 in § 101 in Landau and Lifshitz, 1987). The offset distance between the shock and the piston always increases in time, *i.e.*, the shock is faster than the piston. Shocks of this kind are called piston-shocks. A special case of the piston-shock is the situation where the wave is driven only temporarily, *i.e.*, after the acceleration phase the piston starts decelerating and stops after certain time. The outcome is a freely-propagating shocked simple-wave.

Bearing in mind the above, it can be concluded that the source region expansion caused by the flare energy release would always act as a temporary piston. A shock created in this way, especially in the case of an explosion-like process driven by a pressure pulse, is often denoted as blast wave or simple-wave shock. On the other hand, the CME-driven shock is a combination of the bow-shock and piston-shock: the CME moves through the ambient plasma (projectile effect), but at the same time its body expands in all directions (3D piston effect). However, it is quite likely that the shock formation phase is governed by the 3D piston effect, because in the early phase of the eruption the 3D expansion dominates.

Regarding the physical nature of the driver, we need to specify what we have in mind when making a distinction between flares and CMEs, since the term CME is defined through coronagraphic observations, which generally do not cover the height range where the eruption starts and which is relevant for the formation of coronal shocks. Thus, observations of the CME initiation most often rely on non-coronagraphic data, *i.e.*, imaging in, *e.g.*, the Hα spectral line, or in the EUV and soft X-ray range. The kinematics of an eruption is determined by tracing its early signatures, most often the eruptive prominence and occasionally overlying EUV or soft X-ray coronal features. Observations of this type reveal upward accelerating coronal structures, whose morphology and kinematics match the later white-light CME data (*e.g.*, Plunkett *et al.*, 2000; Srivastava *et al.*, 2000; Vršnak *et al.*, 2004; Gallagher *et al.*, 2003; Maričić *et al.*, 2004; Zhang *et al.*, 2004).

The CME may, or may not be associated with the appearance of a solar flare. By the term flare we have in mind a powerful energy release dominated by non-thermal particles, resulting in hard X-ray emission, as well as impulsive plasma heating that causes the soft X-ray burst. In contrast to the CME, which develops from its early stages to a large-scale coronal disruption and propagates into interplanetary space, the hot flare plasma remains a low-corona phenomenon. Note that, by our definition, a considerable fraction of CMEs will have only very weak (or no) flare signature. Conversely, there are many flares without any signature of a CME ("confined flares").

In many events, however, the CME and a flare are tightly related (so-called eruptive flares), the association rate increasing with the importance of the event. Given the complexity of solar magnetic field and plasma flows, as well as the highly non-linear nature of processes occurring in the solar atmosphere, it is not surprising that the relationship is sometimes very complex, and different evolutionary paths can be involved. Yet, in a majority of events the acceleration phase of CME and the flare impulsive phase are roughly synchronized (Zhang *et al.*, 2001; Zhang *et al.*, 2004; Maričić *et al.*, 2007; Temmer *et al.*, 2008). In general, the flare impulsive phase is shorter than the CME acceleration phase, with the CME upward motion starting before the impulsive phase (Maričić *et al.*, 2007).

In such a situation, in particular during the impulsive phase, it is sometimes difficult to disentangle flare motions from CME motions, *i.e.*, to distinguish between "flare expansion" and "CME". However, it is clear that both the CME expansion towards the high corona and the nonthermal/thermal energy release beneath the CME are present, representing two physically different aspects of the eruption. From the physical point of view, both phenomena could be potential sources of coronal waves. The root of the "flare *vs*. CME" controversy lies in the MHD equation of motion, containing two different terms: the Lorentz force (driver of the CME) and the pressure gradient (presumably driving the expansion of hot flare plasma). For example, in CMEs the expansion is driven by the Lorentz force up to large heights, whereas the presumed flare expansion should be driven only temporarily by a pressure pulse. In both cases the wave is formed by magnetoplasma motion perpendicular to the magnetic field that could be considered as a 3-dimensional piston.

Unfortunately, even detailed case studies do not provide an unambiguous answer to the question whether a given coronal wave was driven by a CME or was ignited by a flare. The primary reason is the synchronization of the CME acceleration phase and the impulsive phase of the associated flare (Zhang *et al.*, 2001; Zhang *et al.*, 2004; Vršnak *et al.*, 2004; Maričić *et al.*, 2007; Temmer *et al.*, 2008; for application to the type II problem see Cliver *et al.*, 2004). Given that in this stage of the eruption the flare and early CME signatures often cannot be clearly distinguished, it is not surprising that discussions on the coronal wave origins have been contentious.

3. CME – Flare – Shock Relationship: Observational Overview

3.1. Type II Bursts

In this paper we focus on type II bursts in the metric wavelength range, since there is a consensus that type II bursts at dekameter and longer wavelengths are driven by CMEs (*e.g.*, Cane, Sheeley and Howard, 1987; Gopalswamy *et al.*, 2000). Metric type II bursts start most often around 100 MHz (Nelson and Melrose, 1985), corresponding to the height range in the order of 100 Mm. Even applying high-density coronal models, such as the ten-fold Saito coronal streamer model (Saito, 1970), the 100 MHz plasma-frequency layer corresponds to heights below ≈ 0.5 solar radii, *i.e.*, 350 Mm. Such heights are also consistent with radioheliograph measurements of the height of type II burst radio sources.

Usually, the emission starts several minutes after the flare impulsive phase, and the back-extrapolation of the emission lanes usually points to the interval between the onset and the peak of the energy release (Harvey, 1965; Švestka and Fritzová-Švestková, 1974; Vršnak *et al.*, 1995; Klassen *et al.*, 1999; Vršnak, 2001). The associated radio emission in the decimetric wavelength range is called the type II burst precursor (Klassen *et al.*, 1999). Sometimes, an intermittent spiky/patchy radio emission, connecting the precursor and type II burst, can be recognized in the dynamic spectrum (Karlický, 1984; Kołomański *et al.*, 2007).

The aforementioned relationship between the type II burst and the impulsive phase of the associated flare is especially well defined in the case of type II bursts with high starting frequencies (say, 300 – 400 MHz). In this type of events the delay of the type II burst onset after the flare peak is in the order of 1 min, so the accuracy of the back-extrapolation is better than a few tens of seconds (Vršnak *et al.*, 1995). In this respect, it should be emphasized that the "launch-time" estimated by the back-extrapolation of emission lanes, is practically independent of the coronal density model used to calculate the radio-source height and speed; a higher-density model results in larger heights, but also in higher velocities, so the two effects balance each other (Vršnak *et al.*, 1995).

The close time/distance relationship between the type II emission and the flare energy release is usually considered as a strong argument favoring the flare-ignited-shock scenario. However, as stated in Section 2, the flare impulsive phase is often (though not always; Maričić *et al.*, 2007) closely associated with the acceleration phase of the flare-related CME (Zhang *et al.*, 2001; Zhang *et al.*, 2004; Vršnak *et al.*, 2004; Maričić *et al.*, 2007; Temmer *et al.*, 2008). So, bearing in mind that the shock formation is tightly related to the acceleration of the source region boundary (see Section 4.1), the close time/distance relationship between the type II emission and the flare energy release does not *a priori* exclude the CME-scenario of the shock formation (Cliver *et al.*, 2004).

In recent years, support has been accumulating for CME-driven metric type II shocks. The most compelling new evidence has been provided by the UltraViolet Coronagraph Spectrometer (UVCS) on SOHO. To date, three cases (11 June 1998; Raymond *et al.*, 2000; 3 March 2000, Mancuso *et al.*, 2002; and 28 June 2000, Ciaravella *et al.*, 2005), have been reported where a shock, temporally associated with a type II burst, was observed via broadening and intensity changes of UV emission lines in front of a CME. Less direct support for the CME-driver scenario is provided by the scaling of CME kinetic energy with the frequency range of type II emission and the high association of EIT waves with CMEs. Gopalswamy *et al.* (2005, 2006) reported that CMEs associated with type II bursts observed in each of the meter, decametric-hectometric, and kilometric bands were more energetic than those associated with bursts in any single wavelength regime. Biesecker *et al.* (2002) presented evidence that all Extreme-Ultraviolet Imaging Telescope (EIT) waves were associated with CMEs, but not vice versa. Cliver *et al.* (2005) reported that $\sim$70% of "high quality" ($Q = 3$) EIT waves from 1997 March to 1998 June originated in C-class or smaller soft X-ray flares.

The existence of fast CMEs without type IIs presents a difficulty for the CME-driver scenario. This objection has been addressed recently by Michalek, Gopalswamy, and Xie (2007) and Gopalswamy *et al.* (2008) who argue that such cases might be explained in terms of (1) the narrower widths and speeds (lower kinetic energy) of radio quiet CMEs; (2) radio occultation/propagation effects; and (3) variable Alfvén speed in the low-latitude outer corona.

On the flare side of the ledger, Magdalenić *et al.* (2008; this Topical Issue) present a strong case for a flare-ignited metric type II burst on 24 December 1996. They considered a limb-event (thus minimizing projection effects), employed radio images, and used EIT data for low coronal observations, to show that impulsive CME acceleration in this event lagged a type II burst which was well-timed with the associated flare. This is the best documented case we are aware of for a flare-ignited type II burst.

Other recent individual event and statistical studies of the sources of metric type II bursts [Hudson and Warmuth, 2004 (12 events, flare hypothesis favored); Cho *et al.*, 2005 (54 events, at least 70 – 80% could be explained by a CME origin); Pohjolainen and Lehtinen, 2006 (three events, two attributed to flares and one to a CME); Cho *et al.*, 2007 (analysis of one event in terms of a CME origin); Reiner *et al.*, 2007 (a single event with both CME- and flare-related type II emission)] obtained results that are more suggestive than definitive. For example, while Hudson and Warmuth (2004) favor the view that the loop oscillations they report originated in waves generated by flares, they note, "Alternatively, however, since the CME association of the TRACE loop oscillations is even stronger ..., one might consider the CME flow field itself to be the exciter." The main argument then presented against a CME source was that in some cases, the TRACE movies show little evidence for dimming. Similarly, while the statistical results of Cho *et al.* (2005) suggested that most, perhaps all, metric type II bursts had CME drivers, they concluded, "we feel that further examinations by using low coronal observations without any extrapolation of CME kinematics are needed to draw a more definite conclusion on the CME origin of type II bursts." In a subsequent analysis based on the Mauna Loa Solar Observatory low coronal observations, Cho *et al.* (2007) presented clear evidence that type II emission originated in a coronal streamer, but less compelling arguments that the shock originated in a CME. The two type II bursts that Pohjolainen and Leitinen (2006) attribute to flares were associated with slow CMEs but these events originated from an active region near disk center (N13W20) and no projection effects were taken into account. Reiner *et al.* (2007) note that they were "unable to conclusively distinguish ... whether ... [one metric type II] shock originated from CME-related ejecta moving at a slower speed or from a distinct (*i.e.*, flare) shock that originated at a slightly different time." In one notable case (03 November 2003) two sets of authors (Vršnak *et al.*, 2006 and Dauphin, Vilmer, and Krucker, 2006) came to opposite conclusions from detailed analyses of the same data sets, with Vršnak *et al.* (2006) favoring a flare driver and Dauphin, Vilmer, and Krucker (2006) a CME.

Recently, White (2007) has presented preliminary evidence of a non-CME type II burst that occurred on 16 July 2004. No CME was observed for this 3B flare located at S09E32. Both metric and Wind/Waves spectrograms show no significant emission (other than type II), consistent with a noneruptive flare. On the other hand, the X3.6 soft X-ray flare had a long ($\sim$5 hr) duration, normally a strong indicator of a CME (Sheeley *et al.*, 1983; see also Andrews, 2003). In addition, a small, slowly developing dimming region formed to the northwest of the active region, which generally indicates the occurrence of a CME (*e.g.*, Thompson *et al.*, 2000; Harrison *et al.*, 2003).

Occasionally, two (or more) type II bursts are observed in close time sequence during a solar eruption (Shanmugaraju *et al.*, 2005; Subramanian and Ebenezer, 2006; Vršnak *et al.*, 2006; Magdalenić *et al.*, 2008). This could be taken as an argument for the existence of flare-ignited shocks, since coronagraphic observations do not show evidence of two (or more) successive CMEs appearing only a few minutes apart. The straightforward explanation of successive type II bursts is either that they are caused by successive bursts of energy release in the flare, or that one shock is due to the CME, whereas the other one is ignited by the flare energy release (Reiner *et al.*, 2000; Shanmugaraju *et al.*, 2005; Subramanian and Ebenezer, 2006; see also Wagner and MacQueen, 1983 and Gary *et al.*, 1984). However, the phenomenon of successive type II bursts can be also explained within the CME-scenario, presuming that the CME-driven shock excites the type II burst emission at different times at widely separated locations (Raymond *et al.*, 2000).

Given the aforementioned situation, where for each argument an opposing explanation can be set forth, it becomes obvious that no firm conclusion can be drawn without a detailed analysis of radioheliographic measurements of the kinematics of the type II burst source relative to the CME kinematics. Especially important are events where the type II radio source is located behind the leading edge of the CME and shows kinematics different from the CME, since this indicates that the shock is probably ignited by the flare. One such event was analyzed in detail by Wagner and MacQeen (1983), who used the Culgoora radioheliograph data to follow the motion of the source of the 17 April 1980 type II burst relative to the associated CME observed by the coronagraph on board the *Solar Maximum Mission*. They found out that the radio source was located well below the top of the white light-transient before the event has reached the height of two solar radii, and that the shock was considerably faster than the CME. Consequently, they concluded that the type II burst emission is independent of the CME and that the shock was probably ignited by the flare. According to their interpretation, the shock was propagating through the already-existing transient disturbance and that the radio emission is excited "when the flare shock overtakes, first, the region of principal density pile-up along the sides of the expanding transient and only later the top of the transient". It is interesting to note that very similar conclusion was reached by Vršnak *et al.* (2006) who used the Nancay Radioheliograph observations of the 3 November 2003 event, and that Leblanc *et al.* (2001) inferred a similar scenario based on a detailed analysis of dynamic spectra of several type II bursts.

However, it should be noted that situations in which the source is found behind the CME leading edge are sometimes explained by presuming that the radio emission is excited at the shock flanks (Steinolfson, 1984; Mancuso and Raymond, 2004). This might be related to the fact that the type II burst source is localized, implying that some special condition must be met for an efficient radio emission. One possibility is, *e.g.*, that the emission is excited only at quasiperpendicular shock segments, where electrons are easily accelerated (see, *e.g.*, Holman and Pesses, 1983; Steinolfson, 1984; Mann and Klassen, 2005). Such conditions are expected to be met aside the flare/CME (Stewart and Magun, 1980; Steinolfson, 1984; Mancuso and Raymond, 2004).

The presented overview of *pro* and *contra* arguments illustrates that statistical (*e.g.*, timing) analyses, as well as most case studies, often do not lead to a straightforward and unambiguous conclusions about the origin of coronal waves. Obviously, a meticulous and systematic analysis of data covering various spectral ranges is required. Furthermore, the observational outcome should be complemented by a careful consideration of the theoretical constraints. For this reason we provide in Section 4 a compact outline of quantitative constraints, which might be used in practice to resolving whether a given shock signature could be attributed to an ejection or to a flare.

3.2. Moreton Waves

Typically, Moreton waves appear as arc-shaped chromospheric disturbances, propagating away from the flare site at speeds in the order of 1000 $\mathrm{km\,s^{-1}}$. The wavefronts are seen in emission in the center and the blue wing of the Hα line, whereas in the red wing they appear in absorption. This is interpreted as a compression and subsequent relaxation of the chromosphere, due to the increased pressure behind the coronal shock sweeping over the chromosphere (Uchida, 1968; Vršnak *et al.*, 2002a).[1] Such a behavior strongly favors the interpretation in terms of freely propagating large-amplitude "simple-wave" (for the physical background see § 102 in Landau and Lifshitz, 1987). Further supporting evidence for such an interpretation is found in the deceleration of the wavefront, elongation of the perturbation profile, and decreasing amplitude of the disturbance (Warmuth *et al.*, 2001; Warmuth *et al.*, 2004b).

In this respect it should be emphasized that there are two ways to form a simple-wave shock pattern. The straightforward option is the formation of the shock by a temporary 3D piston effect, which can be caused either by the flare-volume expansion, or by the initial lateral expansion of the CME. On the other hand, distant flanks of a bow shock also have simple-wave characteristics (Landau and Lifshitz, 1987).

Moreton waves almost always propagate only within a certain angular span; until now, only two 360° events have been observed: on 28 October 2003 (Pick *et al.*, 2005) and on 13 December 2006 (see at http://apod.nasa.gov/apod/ap061213.html). In the study by Warmuth *et al.* (2004a), all 12 of the wave-associated flares from their sample were located at (or extended to) the active region periphery, and the wave propagated away from the active region (see Figure 1 of Warmuth *et al.*, 2004a) [for an example considering type II bursts see Klein *et al.*, 1999]. This suggests that flares which occur in the core of the active region and do not have remote extensions towards quiet regions away from sunspots, are not likely to cause a Moreton wave.

The Moreton wavefront usually becomes detectable at distances in the order of 100 Mm from the source region, most often becoming clearly recognizable in the range 100 – 150 Mm (Warmuth *et al.*, 2001, 2004b). Similar to high-frequency type II bursts, the Moreton wave appearance is closely associated with the flare impulsive phase, usually being delayed by a few minutes. Thus, the onset of the type II burst and the Moreton wave appearance are closely linked, implying that the Moreton wave becomes prominent only after the shock has been formed. Such a short time/distance for shock formation requires an extremely impulsive acceleration of the source region (see below; see also Vršnak and Lulić, 2000; Žic *et al.*, 2008). Since the source region expansion has to be accelerated to a velocity in the order of 1000 $\mathrm{km\,s^{-1}}$ within a minute or so, this requirement favors the flare scenario, since flares typically develop on a shorter time scale than CMEs.

Nonetheless, the application of the Zhang *et al.* (2001) low coronal study to type II bursts by Cliver *et al.* (2004) has similar implications for Moreton waves: CMEs can arise on active region spatial scales with an acceleration scales that mimic those of impulsive flares.

[1] Sometimes even an oscillatory relaxation is observed (Warmuth *et al.*, 2004b; Balasubramaniam, Pevtsov, and Neidig, 2007), which might give the false impression of two or more successive wavefronts.

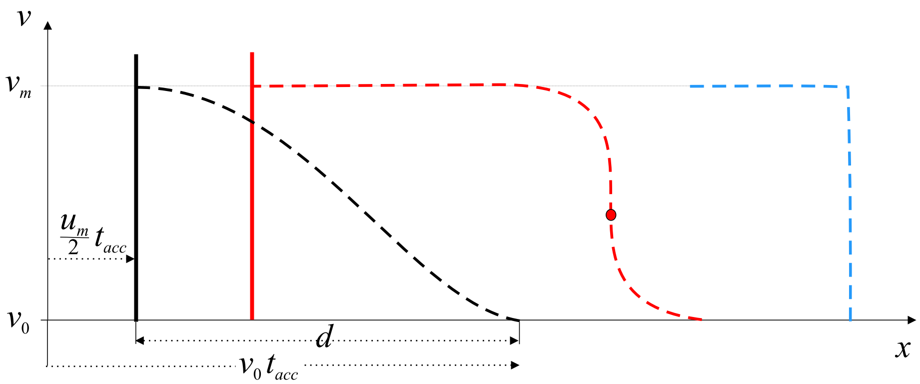

Figure 1 Schematic drawing of wavefront profile steepening and shock formation. The y-axis represents the phase velocity of wavefront elements. The black-dashed line and the bold-black solid line depict, respectively, the wavefront profile and the piston position at $t = t_{\mathrm{acc}}$. The appearance of the discontinuity is indicated by the red dot on the red-dashed profile. The completed shock is drawn by the blue-dashed line.

4. Shock Formation Process

4.1. Nonlinear Wave Evolution

In general terms, the formation of a shock wave requires some source motion that creates a large-amplitude perturbation in the ambient plasma. Such a disturbance transforms into the shock wave due to the nonlinear evolution of the wavefront profile. This happens because the wavefront elements created at later times, *i.e.*, at higher source speed, have larger amplitude and propagate faster than elements formed earlier, at lower source velocity. Consequently, after a certain time a discontinuity forms, *i.e.*, the shock appears, at the perturbation segment where the initial wavefront profile had the steepest slope (Figure 1; for details see Mann, 1995; Vršnak and Lulić, 2000).

Setting the source region boundary (the driver) into motion inevitably requires some acceleration before achieving a given velocity (not only due to inertia, but also due to finite growth-rate of the instability that drives the motion). Thus, the initial wave-front profile is not a discontinuity, but has a finite slope, no matter how impulsive the source acceleration is. Consequently, there is always a certain delay of shock formation after the beginning of the driver expansion, implying also that the shock appears at a certain distance from the source region boundary. A more impulsive acceleration of the driver creates a steeper initial wave-front profile, so faster elements of the profile (elements of larger amplitude) catch up to the slower ones sooner. Consequently, the time needed for the shock formation and the corresponding offset distance are shorter (Mann, 1995; Vršnak and Lulić, 2000; Žic *et al.*, 2008).

The time/distance needed for shock formation can be approximately estimated by considering the 1D piston.[2] Let us assume that the acceleration time profile of the piston is symmetric, so the distance traveled by the piston during the acceleration period t_{acc} is $x_p = u_{\mathrm{m}} t_{\mathrm{acc}}/2$, where u_{m} is the maximum piston velocity. At the same time, the farthermost perturbation

[2]In the case of a cylindrical or spherical piston the shock formation lasts somewhat longer due to the decreasing amplitude of the radially expanding perturbation; see Žic *et al.* (2008).

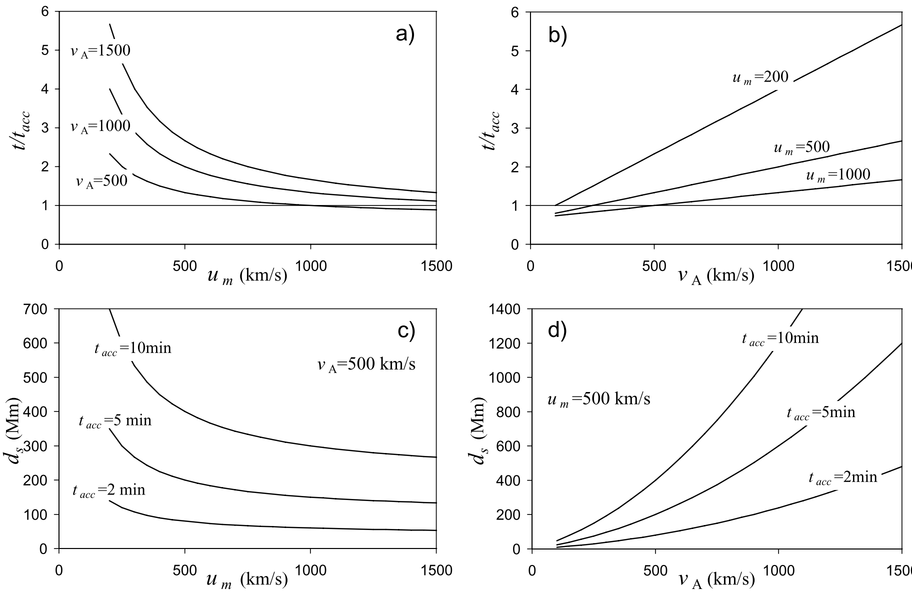

Figure 2 The shock-formation time t_s expressed in units of t_{acc} shown as a function of (a) maximum piston speed u_m (b) ambient Alfvén velocity v_{A0}. The corresponding shock-formation distances calculated applying $t_{acc} = 2$, 5, and 10 min are presented in (c) and (d) for $v_{A0} = 500\ \mathrm{km\,s^{-1}}$ and $u_m = 500\ \mathrm{km\,s^{-1}}$, respectively.

segment has traveled the distance $x_w = v_0 t_{acc}$, where v_0 is the ambient magnetosonic speed. Thus, the wavefront width at the time t_{acc} is $d = x_w - x_p = t_{acc}(v_0 - u_m/2)$. The situation at t_{acc} is drawn in Figure 1, where solid-black vertical line represents the piston position and the dashed-black curve represents the perturbation profile $v(x)$.

The phase velocity v of a given wavefront element is a function of the associated flow velocity u (hereinafter “amplitude”). In the case of low plasma-to-magnetic pressure ratio, $\beta \ll 1$, one can take $v = v_{A0} + 3u/2$ (Mann, 1995; Vršnak and Lulić, 2000), where we have taken into account that in the $\beta \ll 1$ case the magnetosonic speed v_0 reduces to the Alfvén speed v_{A0}. So, the phase velocity of the wavefront element “emitted” at t_{acc} can be expressed as $v_m = v_{A0} + 3u_m/2$.

The shock formation starts with the appearance of the discontinuity in the wavefront profile (depicted by the red dot at the red-dashed curve in Figure 1). The shock formation is completed (blue-dashed curve) when the wavefront element launched at t_{acc}, having the largest phase velocity, v_m, reaches the signal emitted at $t = 0$. Following this consideration, the time of the shock completion can be estimated roughly as

$$t_s \approx t_{acc} + \frac{d}{v_m - v_{A0}} \approx \left[1 + \frac{v_{A0} - u_m/2}{v_m - v_{A0}}\right] t_{acc}. \quad (1)$$

Thus, the delay of the shock formation after the onset of the piston acceleration, t_s, is proportional to t_{acc}. The dependencies $t_s(u_m)$ and $t_s(v_{A0})$ are presented in Figure 2(a) and (b), where t_s is expressed in units of t_{acc}. Figure 2(a) and (b) shows that t_s/t_{acc} is smaller for higher piston speed and lower Alfvén velocity. This also implies that t_s is shorter for higher piston accelerations and Mach numbers. Furthermore, from Figure 2(a) and (b) we find that the shock formation time is comparable with the piston acceleration time ($t_s/t_{acc} \approx 1$) only if the piston achieves Mach numbers around $M_A \approx 1$. In the case of low Mach numbers the shock formation time becomes considerably longer than the piston acceleration phase. Thus, the shock can be formed on a time scale of minutes only if the source region expansion achieves the velocity in the order of Alfvén speed within a few minutes.

Equation (1) also defines the distance at which the shock formation is completed; the distance from the initial piston position is $d_s \approx v_{A0} t_s$. The dependencies $d_s(u_m)$ and $d_s(v_{A0})$ are presented in Figure 2(c) and (d) for $t_{acc} = 2$, 5, and 10 min. Inspecting Figure 2(c) and (d) we find that the shock can form within the range of 100 – 200 Mm (the typical distances of the appearance of Moreton waves and high-frequency type II bursts) only if the piston achieves the speed of at least several hundreds $\mathrm{km\,s^{-1}}$ within a few minutes, in a relatively low Alfvén velocity environment.

Note that in Figure 2(b) and (d) we presented only the results for v_{A0} up to 1500 $\mathrm{km\,s^{-1}}$ although in the core of active regions the Alfvén velocity can be much higher, even larger than 10 000 $\mathrm{km\,s^{-1}}$. However, at such a high value of v_{A0} the shock would be formed at too large distances to cause a Moreton wave and/or a high-frequency type II burst. On the other hand, we emphasize again that the Moreton wave associated flares usually occur at the periphery of active regions where the Alfvén velocity is probably lower than 1000 $\mathrm{km\,s^{-1}}$.

4.2. The Source Region Expansion

The results presented in Section 4.1 indicate that the high-frequency type II bursts and Moreton waves are not likely to be generated by CMEs, since the CME acceleration phase is generally longer than 10 min (Zhang, 2005; Zhang and Dere, 2006; Vršnak *et al.*, 2007), and that is much too long to cause a shock within a few minutes (Figure 2). On the other hand, the flare impulsive phase often consists of a number of distinct energy release episodes developing on the scale of a minute. Assuming that the flare-associated source region expansion is characterized by the same time-scale, and given that the shock formation time is comparable to the source-region acceleration phase (Figure 2), it can be concluded that such an energy release episode could be viable of creating a shock within the required time/distance.

However, considering the flare scenario, we meet another type of problem. Since the active region corona is generally characterized by a low plasma-to-magnetic pressure ratio β (in the active region core it can go down to $\beta \lesssim 10^{-4}$), it is not clear whether the pressure pulse associated with the flare energy release could generate a sufficient source region expansion. So, we have to inspect how the flare loops should react to the pressure pulse, and under which conditions the effect is strong enough to cause a shock.

In the following we present the simplest possible consideration, based on the fact that there are flare loops containing hot plasma (loops rooted in Hα/hard-X-ray emitting regions), and nearby loops which are not affected by the energy release (no flare emission at the loop footpoints). Thus, our consideration is independent of any specific magnetic field geometry, the nature and location of the energy release, or the mechanism by which the energy was transported into the considered plasma volume. The only assumption is that strong pressure gradient develops between the two regions after the impulsive heating of flare loops. In the following we inspect if, and under what condition, such a pressure gradient can drive a plasma motion sufficiently strong to generate a shock wave in the ambient corona.

The considered situation is outlined in Figure 3. The shaded region depicts impulsively heated plasma (darker means hotter), where for the matter of simplicity, we assume that the temperature is approximately constant along field lines and that initially the magnetic field is homogeneous locally. The field lines associated with hot plasma map to the primary energy release site and to the chromospheric flare kernels. The non-shaded region represents the

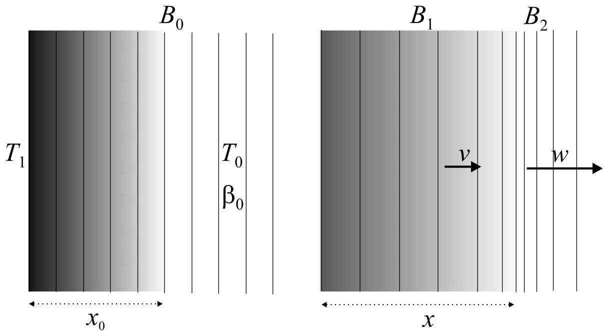

Figure 3 Lateral expansion of an impulsively heated flare loop.

volume which is not connected to the energy release, so the associated plasma is not heated. The pressure gradient exerts the unit-volume force $f_p = \mathrm{d}p/\mathrm{d}x = \rho a$, where ρ is the plasma density. Taking into account that the pressure in flare loops, p, is much higher than in the ambient plasma, and approximating $\rho = nm_p$, where n is the proton number density and m the proton mass, we can write for the initial acceleration $a \approx p/\rho x_0 \approx k_\mathrm{B}T/m_p x_0 \approx c_\mathrm{s}^2/x_0$, where k_B is the Boltzman constant and c_s is the sound velocity in the flaring volume.

Since hot loops are rooted in the flare kernels, the length-scale x_0 over which the pressure p changes should be comparable to the kernel size, which is typically in the order of 10 arcsec or smaller (*e.g.*, Fletcher *et al.*, 2007). Employing the order of magnitude value $x_0 \lesssim 10$ Mm as an upper limit, and taking into account that the temperature of flare loops is several 10^7 K (Aschwanden, 2004) we find that the initial pressure-gradient acceleration could be tremendously high, ranging from $a \approx 10$ to $100\ \mathrm{km\,s^{-2}}$.

On the other hand, the expansion of the source region, *i.e.*, the impulsively heated parts of flare loops, very soon becomes suppressed by the associated magnetic field changes. Since we assume that the magnetic field, B_0 is homogeneous initially (Figure 3, left), and bearing in mind the "frozen-in" condition and the magnetic flux conservation, the magnetic field within the expanding source-region volume should decrease as $B_1 \approx B_0 x_0/x$, where x is the coordinate of the source-region boundary (so-called contact surface). Furthermore, the magnetic pressure increases in front of the source region due to the wave-associated compression caused by the contact-surface motion. Thus, the resulting magnetic pressure gradient can be estimated as $(B_2^2 - B_1^2)/2\mu_0 x$, where the wave-associated compression B_2/B_0 is a function of the contact-surface velocity and the coronal plasma-to-magnetic pressure ratio β_0.

The acceleration stops ($a = 0$) when the internal and external total pressures equalize:

$$\frac{B_2^2}{2\mu_0} = p_1 + \frac{B_1^2}{2\mu_0}, \tag{2}$$

where B_1 and B_2 represent magnetic field behind and ahead of the contact surface, p_1 is the pressure in the flare loop, and we neglected external pressure since we assume that the coronal plasma-to-magnetic pressure ratio is $\beta_0 \ll 1$. Note that at $a = 0$ the source region boundary continues to move, but the acceleration becomes negative, due to further decrease of B_1. So, the boundary decelerates until eventually the expansion stops, which is continued by the contracting motion due to inward directed pressure-gradient force.

Dividing Equation (2) by the unperturbed value of magnetic field pressure, $B_0^2/2\mu_0$, we find

$$\frac{B_2^2}{B_0^2} = \frac{n_1 T_1}{n_0 T_0}\beta_0 + \frac{x_0^2}{x^2}, \tag{3}$$

where the subscript 0 denotes the value in the unperturbed corona, and we have assumed uniform expansion of the source region, $B_1 x = B_0 x_0$.

The wave-associated compression ahead of the contact surface $X = B_2/B_0$ is related to the Alfvén Mach number of the wave propagation, $M_A = (X(X+5)/2(4-X))^{1/2}$ (for details see Priest, 1982; see also Appendix in Vršnak *et al.*, 2002b). Thus, the pressure increase in flaring loops ($n_1 T_1/n_0 T_0$) is directly related to the amplitude of the emitted wave (B_2/B_0). Equation (3) shows that larger wave amplitudes are achieved for higher pressure increase. Furthermore, if the condition $\beta_0 \to 0$ is considered, we find that $x/x_0 \to 1$ since in the case of expansion the condition $B_2 > B_0$ must be satisfied. This implies that at very low β_0 there is practically no expansion ($x \approx x_0$) and no shock formation ($B_2 \approx B_0$). Thus, a shock can be formed only if β_0 is not too low, and the pressure increase is sufficiently high.

In this respect it is important to note that type II burst shocks are characterized by relatively low amplitude. They propagate at Mach numbers generally below $M_A < 2$ (Nelson and Melrose, 1985; see also Hudson *et al.*, 2003), having mean amplitude around $X \approx 1.5$ (see Figure 3 of Vršnak *et al.*, 2002b). Another important point is, as emphasized in Section 3.2, that flares associated with Moreton waves are usually located at (or have extensions to) the active region periphery, so it can be assumed that actual value of β_0 is larger than in the active region core, where it can be as low as $\beta \lesssim 10^{-4}$. We note that the magnetic field decreases rapidly with the distance from the active region core (*e.g.*, Figures 4 and 5 in Warmuth and Mann, 2005), becoming around two orders of magnitude lower than in sunspots already ~ 50 Mm from the core, which corresponds to four orders of magnitude larger β than in central parts of the active region (for a discussion regarding the problem of plasma β we refer to Gary, 2001).

The flare-loop temperature can be as large as 4×10^7 K (Aschwanden, 2004), so we can take $n_1 T_1/n_0 T_0 > T_1/T_0 = 10-40$, since the density of flare loops is also increased with respect to quiet corona (Aschwanden, 2004). For purpose of illustration, let us take $\beta_0 = 0.1$ and $n_1 T_1/n_0 T_0 = 20$ and require the wave amplitude $X = 1.5$, corresponding to the Alfvén Mach number $M_A = 1.4$). From Equation (3) we find that in such a case the source region has to expand to $x \approx 1.9 x_0$. Using the relationship between the plasma flow velocity and the associated wave speed (see Section 4.1; for details we refer to Vršnak and Lulić, 2000), we find that the contact-surface velocity, corresponding to the wave Alfvén Mach number of $M_A = 1.4$, is equal to $u \approx 0.27 v_A$. Taking the order of magnitude value $v_A \approx 1000$ km s^{-1} and the order-of-magnitude upper limit $x_0 = 10$ Mm, this corresponds to the mean acceleration of $a = v^2/2(x - x_0) \approx 4$ km s^{-2} and the acceleration time of $t_a = v/a \approx 1$ min. Higher values of v_A and/or smaller x_0 would increase the value of a and reduce t_a. If one would require $M_A = 2$ at the same value of β_0, a stronger pressure pulse and shorter expansion length would be needed. For example, taking, *e.g.*, $n_1 T_1/n_0 T_0 \approx 40$ we find $x/x_0 \approx 1.4$. The latter effect implies also a very impulsive acceleration ($a \approx 50$ km s^{-2} over $t_a \approx 15$ s). At lower value of β_0, *e.g.*, $\beta_0 = 0.01$, the required pressure increase becomes larger than allowed by observations.

The above order of magnitude analysis shows that the flare-associated pressure pulse cannot ignite the shock wave in strong field regions characterized by very low β. The mechanism requires a relatively high value of the plasma-to-magnetic pressure ratio, $\beta_0 \approx 0.1-0.01$, and low Alfvén velocity. This might explain why only a very small fraction of flare/CME events cause coronal shocks, why Moreton waves are launched by eruptions that are located at the active region outskirts, and why type II burst shocks have low amplitudes.

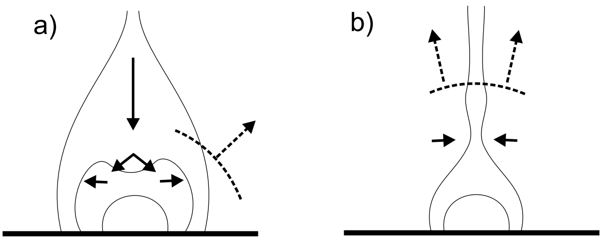

Figure 4 (a) Magnetic pressure pulse caused by the formation of the reconnection outflow and the associated deformation of low-lying loops. (b) Outward moving perturbation created by the changing reconnection rate. Shock waves are depicted by dashed arcs, plasma flows by bold arrows, and field lines by thin solid lines.

4.3. Reconnection-Related Alternative Options

We note that the pressure pulse might not be the only viable flare-related mechanism of the shock formation. In Figure 4(a) and (b) we sketch two additional scenarios, which are quite speculative at this level, but are worth mentioning, since they are closely related to results of numerical simulations. The first one is related to the formation of a downward-directed reconnection jet, which may or may not be supersonic (for a discussion see Bárta, Vršnak, and Karlický, 2008, and references therein). Although in Figure 4(a) and (b) we employ cartoons such as used to depict two-ribbon flares, the following consideration can be applied to any other specific reconnection geometry. After reconnection sets-in at certain height in the corona, the reconnection jet propagates downward (Bárta *et al.*, 2007), until reaching the low-lying loops (Figure 4(a)). The "impact" deforms the loops (even in the subsonic case), forcing their sideways expansion, and if the expansion is impulsive enough, it might create a fast-mode shock wave in the ambient corona. Furthermore, we note that in the course of the reconnection process, the formation of current-sheet plasmoids is expected. Numerical simulations show that some plasmoids move downward and coalesce with previously formed flare loops (Forbes and Priest, 1983; Bárta, Vršnak, and Karlický, 2008; Riley *et al.*, 2007). The interaction creates a powerful energy release and strong deformation of loops (Bárta, Vršnak, and Karlický, 2008), which can result in the formation of a large-scale coronal wave (see a series of waves in Figure 3 – animation in Riley *et al.*, 2007). However, note that there is little observational evidence for reconnection downflows (see discussion in Bárta, Vršnak, and Karlický, 2008, and references therein), especially during the impulsive phase. Even when downward motions are observed (for the impulsive phase see Asai *et al.*, 2004), their nature is not clear. Yet, as demonstrated by Asai *et al.* (2004) the downflows show significant deceleration, implying they transfer the momentum to the low-lying structures.

In Figure 4(b) we sketch the shock formation associated with a variable reconnection rate. The propagation of a large-amplitude wave along the current sheet, related to the change of reconnection rate, was anticipated by Volonskaya *et al.* (2003). Recently, such a wave was revealed in the numerical simulation by Bárta *et al.* (2007). However, we note that while such quasi-longitudinal shocks could explain type II bursts, it is not likely that they could create Moreton waves, since the flanks of the shock probably do not reach the chromospheric layers (see Figure 3 of Bárta *et al.*, 2007). Finally, we recall numerical experiments by Forbes (1988) and Karlický (1988), where quasiperpendicular fast-mode shocks were launched directly from the diffusion region after the onset of the fast reconnection stage.

5. Discussion: Flares or CMEs?

The presented consideration of the shock formation process indicates that coronal shocks causing high-frequency type II bursts and Moreton waves could be caused by the energy release in flares or by extremely impulsive CMEs. In the following we summarize advantages and drawbacks of the flare and CME scenarios.

The kinematics of CMEs is certainly compatible with the formation of coronal shocks causing type II bursts in the meter-to-dekameter wavelength range. However, the situation is not so clear for shocks causing high-frequency type II bursts and Moreton waves since the required acceleration is more impulsive than usually observed in CMEs. Although it was demonstrated in Section 4.1 that the piston mechanism does not require supermagnetosonic speeds, the CME still has to achieve a velocity of several hundreds of $\mathrm{km\,s^{-1}}$ within a few minutes (Figure 2). This implies that the acceleration has to be larger than 1 $\mathrm{km\,s^{-2}}$, which is observed only in the most impulsive CMEs. From a theoretical point of view such accelerations should not be a problem, since accelerations up to 10 $\mathrm{km\,s^{-2}}$ could be expected if a compact magnetic structure (size on the order of 100 Mm) is launched from strong magnetic field regions (Vršnak *et al.*, 2007). In this respect, one should keep in mind that observations are often hampered by insufficient time resolution in the field of view of interest (especially in the case of disc observations), *i.e.*, the most impulsive ejections could easily be missed by the full-disc low-corona patrol (like EIT) because of a too low time resolution. We note that the six type II-associated CMEs in November 1997 analyzed by Cliver *et al.* (2004) had average inferred accelerations (CME speed divided by flare rise time; following Zhang *et al.*, 2001) ranging from 756 to 6483 $\mathrm{m\,s^{-2}}$ (median $\sim 2000\ \mathrm{m\,s^{-2}}$).

The impulsive phase of flares is characterized by considerably shorter time scales than the CME acceleration stage. The energy release episodes develop on a scale of minutes, which is compatible with requirements posed by the observed shock formation distances. Furthermore, the observed timing (including the back-extrapolation of the shock kinematics) is fully consistent with the flare scenario. We emphasize that this relationship is not yet appropriately investigated in the case of CMEs. The main problem lies in the fact that measurements of sufficient quality to allow deriving the acceleration time-profile are quite rare, so there are only few case studies that include both the kinematics of the shock and the acceleration-curve of the ejection (*e.g.*, Vršnak *et al.*, 2006; Liu *et al.*, 2007). Statistical studies show no (Reiner *et al.*, 2001) or only a weak (Shanmugaraju *et al.*, 2003; Mancuso and Raymond, 2004) correlation of CME speeds and shock velocities inferred from type II burst frequency-drifts. On the other hand, well-defined correlations have been obtained between flare parameters and shock characteristics that are consistent with the flare scenario (Vršnak, 2001, and references therein). However, even here, ambiguity remains. For example, the finding that starting frequencies of type II bursts are higher for impulsive flares can be explained in the CME scenario by the fact that short flare time scales indicate a small initial spatial scale for a CME, thus enabling it to drive type II shocks lower in the corona.

There are some serious drawbacks related to the flare scenario. The most serious one is related to the large discrepancy in occurrence rate of flares and observable coronal shocks, *i.e.*, only a small number of flares (even if small flares are excluded) causes large-scale waves (Cliver, Webb, and Howard, 1999). Although this drawback burdens also the CME scenario, it is not so problematic in the case of CMEs, since all gradual events could be excluded a priori. Obviously, if flares can produce coronal shocks, there must be a very stringent special condition(s) which does not allow the shock formation in the majority of events. Given the high degree of association of type II bursts with CMEs, and keeping in mind the results presented in Section 4, one possibility is that only dynamical ("two-ribbon") flares, occurring at preferable locations, produce shocks. There exist intense, impulsive, confined flares (*e.g.*, Gopalswamy *et al.*, 1995; *cf.*, Benz, Brajša, and Magdalenić, 2007) that lack any associated metric-wavelength emission; such events would seem ideal candidates to produce blast-wave type II bursts. Recently, Chen (2006) examined EIT observations for 14 non-CME-associated energetic ($\geq$M1.0) flares occurring near solar minimum, and found that none had associated EIT waves. He concluded that it was therefore unlikely that flare pressure pulses generate such waves.

Theoretical considerations indicate that low Alfvén velocity in the ambient plasma and relatively high plasma-to-magnetic pressure ratio in the source region ($\beta \approx 0.01-0.1$) are favorable conditions for the shock formation. This implies that only flares extending to the active region periphery are likely to ignite the shock, which is in fact consistent with observations. This is also compatible with the previously mentioned condition, since such a situation more easily occurs in the case of dynamical flares, because the associated CMEs usually include eruption of magnetic structures that extend out of active regions.

Another difficulty with the flare scenario concerns the source-region expansion, which is not directly observed. However, we should keep in mind that the expected/required expansion is on the order of 10 Mm (Section 4). Such a short-range (and extremely impulsive) expansion cannot be recognized with currently operating soft X-ray imaging instruments.

6. Conclusion: Impasse and Suggestions

Sixty years after the discovery of slow-drift radio bursts in the solar corona by Payne-Scott, Yabsley, and Bolton (1947), the debate about the origin of metric type II bursts continues. In Section 3 we surveyed various observational facts, interpretations, and opinions, to illustrate a rather chaotic state of the art.

To summarize, the existence of CME-generated type II bursts is not in question. It is generally accepted that all interplanetary (kilometric) type IIs (Sheeley *et al.*, 1985; Cane, Sheeley, and Howard, 1987), many (if not all) decametric-hectometric type IIs (Gopalswamy *et al.*, 2000), and at least some metric type II bursts (*e.g.*, Raymond *et al.*, 2000; Cane and Erickson, 2005) are CME generated. On the other hand, the existence of "pure" flare-generated type II bursts remains to be demonstrated. Of course, an unambiguous observation of a type II burst originating in a noneruptive flare would provide conclusive evidence that at least some slow-drift bursts arise in this manner.

However, given the high association rate of coronal waves and type IIs with CMEs (Cliver, Webb, and Howard, 1999; Biesecker *et al.*, 2002), and bearing in mind the interpretation by Wagner and MacQueen (1983) and Vršnak *et al.* (2006) that the flare shock excites a type II burst when interacting with the CME "envelope", it is quite likely that CMEs are a necessary condition for the appearance of type II bursts, even if not driving the shock. Thus, the absence of type IIs associated with noneruptive flares does not necessarily imply that flare-ignited shocks do not exist.

How to resolve the impasse? We see two promising directions of research, both requiring radioheliograph observations, measurement of kinematics of low-coronal signatures of the CME, and multiwavelength observations of the flare. The first of these directions is to search for type II bursts in which the acceleration phase of the CME and the flare impulsive phase are not synchronized, as was the case in the event reported by Magdalenić *et al.* (2008). In such events the relative kinematics of the CME and the type II burst source should be carefully analyzed, to check if their behavior is consistent with theoretical constraints, such as those given in Section 4.1. For example, knowing the velocity and acceleration time-profile of the ejection, the time/distance at which shock should form can be estimated for a certain range of Alfvén velocities, and if the discrepancy between the predicted and measured values is too large, the ejection can be eliminated as a possible source of the wave.

The second option is to focus on the events where the type II burst source is located far behind the CME leading edge, like in the event described by Wagner and MacQueen (1983) and Gary *et al.* (1984). Again, the relative kinematics of the two phenomena should be checked, including the lateral expansion of the CME, and the outcome should be confronted with the theoretical aspect of the problem. In such situations, it is essential to take into account that in the case of a blunt body there is always a certain offset between the shock and the driver (Russell and Mulligan, 2002), and that the geometry of the shock flanks should roughly correspond to the Mach cone.

Finally, in the events proven to be flare-related, a high-cadence Hα, EUV, soft X-ray, and low coronagraph data (when available) should be applied to shed light on the nature of a flare driver, *e.g.*, volume expansion or short-lived/arrested ejecta. Especially important would be to find, until now missing, unambiguous evidence for the presumed expansion of hot loops, and to estimate its range.

Acknowledgements We thank the referee and the guest editor K.-L. Klein for helpful and stimulating comments. E. W. C. acknowledges support from the Window on Europe Program of the Air Force Office of Scientific Research. B. V. acknowledges support by the Air Force Office of Scientific Research, USAF, grant number FA8655-06-1-3036.

References

Andrews, M.D.: 2003, A search for CMEs associated with big flares. *Solar Phys.* **218**, 261 – 279. doi:10.1023/B:SOLA.0000013039.69550.bf.

Asai, A., Yokoyama, T., Shimojo, M., Shibata, K.: 2004, Downflow motions associated with impulsive nonthermal emissions observed in the 2002 July 23 solar flare. *Astrophys. J.* **605**, L77 – L80. doi:10.1086/420768.

Aschwanden, M.J.: 2004, *Physics of the Solar Corona. An Introduction*, Springer, Berlin.

Attrill, G.D.R., Harra, L.K., van Driel-Gesztelyi, L., Démoulin, P.: 2007, Coronal “wave”: magnetic footprint of a coronal mass ejection? *Astrophys. J.* **656**, L101 – L104. doi:10.1086/512854.

Balasubramaniam, K.S., Pevtsov, A.A., Neidig, D.F.: 2007, Are Moreton waves coronal phenomena? *Astrophys. J.* **658**, 1372 – 1379. doi:10.1086/512001.

Bárta, M., Vršnak, B., Karlický, M.: 2008, Dynamics of plasmoids formed by the current sheet tearing. *Astron. Astrophys.* **477**, 649 – 655. doi:10.1051/0004-6361:20078266.

Bárta, M., Karlický, M., Vršnak, B., Goossens, M.: 2007, MHD waves and shocks generated during magnetic field reconnection. *Cent. Eur. Astrophys. Bull.* **31**, 165 – 180.

Benz, A.O., Brajša, R., Magdalenić, J.: 2007, Are there radio-quiet solar flares? *Solar Phys.* **240**, 263 – 270. doi:10.1007/s11207-007-0365-9.

Biesecker, D.A., Myers, D.C., Thompson, B.J., Hammer, D.M., Vourlidas, A.: 2002, Solar phenomena associated with “EIT waves”. *Astrophys. J.* **569**, 1009 – 1015. doi:10.1086/339402.

Cane, H.V., Erickson, W.C.: 2005, Solar type II radio bursts and IP type II events. *Astrophys. J.* **623**, 1180 – 1194. doi:10.1086/428820.

Cane, H.V., Sheeley, N.R. Jr., Howard, R.A.: 1987, Energetic interplanetary shocks, radio emission, and coronal mass ejections. *J. Geophys. Res.* **92**, 9869 – 9874.

Chen, P.F.: 2006, The relation between EIT waves and solar flares. *Astrophys. J.* **641**, L153 – L156. doi:10.1086/503868.

Chen, P.F., Fang, C., Shibata, K.: 2005, A full view of EIT waves. *Astrophys. J.* **622**, 1202 – 1210. doi:10.1086/428084.

Cho, K.S., Moon, Y.J., Dryer, M., Shanmugaraju, A., *et al.*: 2005, Examination of type II origin with SOHO/LASCO observations. *J. Geophys. Res. (Space Phys.)* **110**, A12101. doi:10.1029/2004JA010744.

Cho, K.S., Lee, J., Moon, Y.J., Dryer, M., *et al.*: 2007, A study of CME and type II shock kinematics based on coronal density measurement. *Astron. Astrophys.* **461**, 1121 – 1125. doi:10.1051/0004-6361:20064920.
Ciaravella, A., Raymond, J.C., Kahler, S.W., Vourlidas, A., Li, J.: 2005, Detection and diagnostics of a coronal shock wave driven by a partial-halo coronal mass ejection on 28 June 2000. *Astrophys. J.* **621**, 1121 – 1128. doi:10.1086/427619.
Cliver, E.W., Webb, D.F., Howard, R.A.: 1999, On the origin of solar metric type II bursts. *Solar Phys.* **187**, 89 – 114.
Cliver, E.W., Nitta, N.V., Thompson, B.J., Zhang, J.: 2004, Coronal shocks of November 1997 revisited: The CME type II timing problem. *Solar Phys.* **225**, 105 – 139. doi:10.1007/s11207-004-3258-1.
Cliver, E.W., Laurenza, M., Storini, M., Thompson, B.J.: 2005, On the origins of solar EIT waves. *Astrophys. J.* **631**, 604 – 611. doi:10.1086/432250.
Dauphin, C., Vilmer, N., Krucker, S.: 2006, Observations of a soft X-ray rising loop associated with a type II burst and a coronal mass ejection in the 03 November 2003 X-ray flare. *Astron. Astrophys.* **455**, 339 – 348. doi:10.1051/0004-6361:20054535.
Delaboudinière, J.P., Artzner, G.E., Brunaud, J., Gabriel, A.H., *et al.*: 1995, EIT: Extreme-ultraviolet imaging telescope for the SOHO mission. *Solar Phys.* **162**, 291 – 312.
Delannée, C., Aulanier, G.: 1999, CME associated with transequatorial loops and a bald patch flare. *Solar Phys.* **190**, 107 – 129.
Dodson, H.W.: 1949, Position and development of the solar flares of 8 and 10 May 1949. *Astrophys. J.* **110**, 382 – 386.
Fletcher, L., Hannah, I.G., Hudson, H.S., Metcalf, T.R.: 2007, A TRACE white light and RHESSI hard X-ray study of flare energetics. *Astrophys. J.* **656**, 1187 – 1196. doi:10.1086/510446.
Forbes, T.G.: 1988, Shocks produced by impulsively driven reconnection. *Solar Phys.* **117**, 97 – 121.
Forbes, T.G., Priest, E.R.: 1983, A numerical experiment relevant to line-tied reconnection in two-ribbon flares. *Solar Phys.* **84**, 169 – 188.
Gallagher, P.T., Lawrence, G.R., Dennis, B.R.: 2003, Rapid acceleration of a coronal mass ejection in the low corona and implications for propagation. *Astrophys. J.* **588**, L53 – L56. doi:10.1086/375504.
Gary, G.A.: 2001, Plasma beta above a solar active region: Rethinking the paradigm. *Solar Phys.* **203**, 71 – 86.
Gary, D.E., Dulk, G.A., House, L., Illing, R., *et al.*: 1984, Type II bursts, shock waves, and coronal transients – The event of 29 June 1980, 0233 UT. *Astron. Astrophys.* **134**, 222 – 233.
Gilbert, H.R., Holzer, T.E.: 2004, Chromospheric waves observed in the He I spectral line ($\lambda = 10\,830$ Å): A closer look. *Astrophys. J.* **610**, 572 – 587. doi:10.1086/421452.
Gilbert, H.R., Thompson, B.J., Holzer, T.E., Burkepile, J.T.: 2001, A comparison of CME-associated atmospheric waves observed in coronal (19.5 nm) and chromospheric (He I 1083 nm and H-alpha 656 nm) lines. *AGU Fall Meeting Abstracts*, B746.
Gopalswamy, N.: 2006, *Coronal Mass Ejections and Type II Radio Bursts*, *Washington DC American Geophysical Union Geophysical Monograph Series* **165**, 207–220.
Gopalswamy, N., Raulin, J.P., Kundu, M.R., Nitta, N., *et al.*: 1995, VLA and YOHKOH observations of an M1.5 flare. *Astrophys. J.* **455**, 715 – 732. doi:10.1086/176618.
Gopalswamy, N., Kaiser, M.L., Thompson, B.J., Burlaga, L.F., *et al.*: 2000, Radio-rich solar eruptive events. *Geophys. Res. Lett.* **27**, 1427 – 1430.
Gopalswamy, N., Aguilar-Rodriguez, E., Yashiro, S., Nunes, S., *et al.*: 2005, Type II radio bursts and energetic solar eruptions. *J. Geophys. Res.* **110**, A12 S07. doi:10.1029/2005JA011158.
Gopalswamy, N., Yashiro, S., Xie, H., Akiyama, S., *et al.*: 2008, Radio-quiet fast and wide coronal mass ejections. *Astrophys. J.* **674**, 560 – 569.
Harrison, R.A., Bryans, P., Simnett, G.M., Lyons, M.: 2003, Coronal dimming and the coronal mass ejection onset. *Astron. Astrophys.* **400**, 1071 – 1083. doi:10.1051/0004-6361:20030088.
Harvey, G.A.: 1965, 2800 Megacycle per second radiation associated with type II and type IV solar radio bursts and the relation with other phenomena. *J. Geophys. Res.* **70**, 2961.
Holman, G.D., Pesses, M.E.: 1983, Solar type II radio emission and the shock drift acceleration of electrons. *Astrophys. J.* **267**, 837 – 843. doi:10.1086/160918.
Hudson, H.S., Warmuth, A.: 2004, Coronal loop oscillations and flare shock waves. *Astrophys. J.* **614**, L85 – L88. doi:10.1086/425314.
Hudson, H.S., Khan, J.I., Lemen, J.R., Nitta, N.V., Uchida, Y.: 2003, Soft X-ray observation of a large-scale coronal wave and its exciter. *Solar Phys.* **212**, 121 – 149. doi:10.1023/A:1022904125479.
Karlický, M.: 1984, Narrowband dm-spikes as indication of flare mass ejection. *Solar Phys.* **92**, 329 – 342.
Karlický, M.: 1988, Response of the current sheet to a time-limited enhancement of electrical resistivity. *Bull. Astron. Inst. Czechoslov.* **39**, 13 – 23.
Khan, J.I., Aurass, H.: 2002, X-ray observations of a large-scale solar coronal shock wave. *Astron. Astrophys.* **383**, 1018 – 1031. doi:10.1051/0004-6361:20011707.

Klassen, A., Aurass, H., Klein, K.L., Hofmann, A., Mann, G.: 1999, Radio evidence on shock wave formation in the solar corona. *Astron. Astrophys.* **343**, 287 – 296.

Klein, K.L., Khan, J.I., Vilmer, N., Delouis, J.M., Aurass, H.: 1999, X-ray and radio evidence on the origin of a coronal shock wave. *Astron. Astrophys.* **346**, L53 – L56.

Kołomański, S., Tomczak, M., Ronowicz, P., Karlický, M., Aurass, H.: 2007, Flare-associated X-ray plasma ejections and radio drifting structures. *Cent. Eur. Astrophys. Bull.* **31**, 125 – 134.

Landau, L.D., Lifshitz, E.M.: 1987, *Fluid Mechanics*, 2nd edn., Oxford, Pergamon Press.

Leblanc, Y., Dulk, G.A., Vourlidas, A., Bougeret, J.L.: 2001, Tracing shock waves from the corona to 1 AU: Type II radio emission and relationship with CMEs. *J. Geophys. Res.* **106**, 25301 – 25312. doi:10.1029/2000JA000260.

Liu, C., Lee, J., Yurchyshyn, V., Deng, N., *et al.*: 2007, The eruption from a sigmoidal solar active region on 13 May 2005. *Astrophys. J.* **669**, 1372 – 1381. doi:10.1086/521644.

Magdalenić, J., Vršnak, B., Pohjolainen, S., Temmer, M., Aurass, H., Lehtinen, N.: 2008, Multi-wavelength study of coronal waves associated with the CME-flare event of 24 December 1996. *Solar Phys.* doi:10.1007/s11207-008-9220-x. This issue.

Mancuso, S., Raymond, J.C.: 2004, Coronal transients and metric type II radio bursts. I. Effects of geometry. *Astron. Astrophys.* **413**, 363 – 371. doi:10.1051/0004-6361:20031510.

Mancuso, S., Raymond, J.C., Kohl, J., Ko, Y.K., Uzzo, M., Wu, R.: 2002, UVCS/SOHO observations of a CME-driven shock: Consequences on ion heating mechanisms behind a coronal shock. *Astron. Astrophys.* **383**, 267 – 274. doi:10.1051/0004-6361:20011721.

Mann, G.: 1995, Simple magnetohydrodynamic waves. *J. Plasma Phys.* **53**, 109 – 125.

Mann, G., Klassen, A.: 2005, Electron beams generated by shock waves in the solar corona. *Astron. Astrophys.* **441**, 319 – 326. doi:10.1051/0004-6361:20034396.

Maričić, D., Vršnak, B., Stanger, A.L., Veronig, A.: 2004, Coronal mass ejection of 15 May 2001: I. Evolution of morphological features of the eruption. *Solar Phys.* **225**, 337 – 353. doi:10.1007/s11207-004-3748-1.

Maričić, D., Vršnak, B., Stanger, A.L., Veronig, A.M., Temmer, M., Roša, D.: 2007, Acceleration phase of coronal mass ejections: II. Synchronization of the energy release in the associated flare. *Solar Phys.* **241**, 99 – 112. doi:10.1007/s11207-007-0291-x.

Michalek, G., Gopalswamy, N., Xie, H.: 2007, Width of radio-loud and radio-quiet CMEs. *Solar Phys.* **246**, 409 – 414. doi:10.1007/s11207-007-9062-y.

Moreton, G.E.: 1960, Hα Observations of flare-initiated disturbances with velocities $\approx 1000\ \mathrm{km\,s^{-1}}$. *Astron. J.* **65**, 494 – 495. doi:10.1086/108346.

Moreton, G.E., Ramsey, H.E.: 1960, In: *Recent Observations of Dynamical Phenomena Associated with Solar Flares* **CS-72**, Astron. Soc. Pac., San Francisco, 357 – 358.

Moses, D., Clette, F., Delaboudinière, J.P., Artzner, G.E., *et al.*: 1997, EIT observations of the extreme ultraviolet sun. *Solar Phys.* **175**, 571 – 599. doi:10.1023/A:1004902913117.

Narukage, N., Hudson, H.S., Morimoto, T., Akiyama, S., *et al.*: 2002, Simultaneous observation of a Moreton wave on 3 November 1997 in Hα and soft X-rays. *Astrophys. J.* **572**, L109 – L112. doi:10.1086/341599.

Nelson, G.J., Melrose, D.B.: 1985, Type II bursts. In: *Solar Radiophysics*, Cambridge University Press, Cambridge, 333 – 359.

Neupert, W.M.: 1989, Transient coronal extreme ultraviolet emission before and during the impulsive phase of a solar flare. *Astrophys. J.* **344**, 504 – 512. doi:10.1086/167819.

Payne-Scott, R., Yabsley, D.E., Bolton, J.G.: 1947, Relative times of arrival of solar noise on different radio frequencies. *Nature* **160**, 256 – 257.

Pick, M., Malherbe, J.M., Kerdraon, A., Maia, D.J.F.: 2005, On the disk Hα and radio observations of the 28 October 2003 flare and coronal mass ejection event. *Astrophys. J.* **631**, L97 – L100. doi:10.1086/497137.

Plunkett, S.P., Vourlidas, A., Šimberová, S., Karlický, M., Kotrč, P., Heinzel, P., Kupryakov, Y.A., Guo, W.P., Wu, S.T.: 2000, Simultaneous SOHO and ground-based observations of a large eruptive prominence and coronal mass ejection. *Solar Phys.* **194**, 371 – 391.

Pohjolainen, S., Lehtinen, N.J.: 2006, Slow halo CMEs with shock signatures. *Astron. Astrophys.* **449**, 359 – 367. doi:10.1051/0004-6361:20054118.

Priest, E.R.: 1982, *Solar Magneto-Hydrodynamics*, Reidel, Dordrecht.

Ramsey, H.E., Smith, S.F.: 1966, Flare-initiated filament oscillations. *Astron. J.* **71**, 197 – 199.

Raymond, J.C., Thompson, B.J., St. Cyr, O.C., Gopalswamy, N., *et al.*: 2000, SOHO and radio observations of a CME shock wave. *Geophys. Res. Lett.* **27**, 1439 – 1442. doi:10.1029/1999GL003669.

Reiner, M.J., Kaiser, M.L., Plunkett, S.P., Prestage, N.P., Manning, R.: 2000, Radio tracking of a white-light coronal mass ejection from solar corona to interplanetary medium. *Astrophys. J.* **529**, L53 – L56. doi:10.1086/312446.

Reiner, M.J., Kaiser, M.L., Gopalswamy, N., Aurass, H., *et al.*: 2001, Statistical analysis of coronal shock dynamics implied by radio and white-light observations. *J. Geophys. Res.* **106**, 25279 – 25290. doi:10.1029/2000JA004024.

Reiner, M.J., Krucker, S., Gary, D.E., Dougherty, B.L., Kaiser, M.L., Bougeret, J.L.: 2007, Radio and white-light coronal signatures associated with the RHESSI hard X-ray event of 23 July 2002. *Astrophys. J.* **657**, 1107 – 1116. doi:10.1086/510827.

Riley, P., Lionello, R., Mikić, Z., Linker, J., *et al.*: 2007, "Bursty" reconnection following solar eruptions: MHD simulations and comparison with observations. *Astrophys. J.* **655**, 591 – 597. doi:10.1086/509913.

Russell, C.T., Mulligan, T.: 2002, On the magnetosheath thicknesses of interplanetary coronal mass ejections. *Planet. Space Sci.* **50**, 527 – 534.

Saito, K.: 1970, A non-spherical axisymmetric model of the solar K corona of the minimum type. *Ann. Obs. Astron. Tokyo* **12**, 53 – 120.

Sedov, L.I.: 1959, *Similarity and Dimensional Methods in Mechanics*, Academic Press, New York.

Shanmugaraju, A., Moon, Y.J., Vršnak, B.: 2008, Type II radio bursts with high and low starting frequencies. *Solar Phys.* submitted.

Shanmugaraju, A., Moon, Y.J., Dryer, M., Umapathy, S.: 2003, An investigation of solar maximum metric type II radio bursts: Do two kinds of coronal shock sources exist? *Solar Phys.* **215**, 161 – 184.

Shanmugaraju, A., Moon, Y.J., Cho, K.S., Kim, Y.H., Dryer, M., Umapathy, S.: 2005, Multiple type II solar radio bursts. *Solar Phys.* **232**, 87 – 103. doi:10.1007/s11207-005-1586-4.

Sheeley, N.R. Jr., Howard, R.A., Koomen, M.J., Michels, D.J.: 1983, Associations between coronal mass ejections and soft X-ray events. *Astrophys. J.* **272**, 349 – 354. doi:10.1086/161298.

Sheeley, N.R. Jr., Howard, R.A., Michels, D.J., Koomen, M.J., *et al.*: 1985, Coronal mass ejections and interplanetary shocks. *J. Geophys. Res.* **90**, 163 – 175.

Srivastava, N., Schwenn, R., Inhester, B., Martin, S.F., Hanaoka, Y.: 2000, Factors related to the origin of a gradual coronal mass ejection associated with an eruptive prominence on 21 – 22 June 1998. *Astrophys. J.* **534**, 468 – 481. doi:10.1086/308749.

Steinolfson, R.S.: 1984, Type II radio emission in coronal transients. *Solar Phys.* **94**, 193 – 202.

Stewart, R.T., Magun, A.: 1980, Radio evidence for electron acceleration by transverse shock waves in herringbone Type II solar bursts. *Proc. Astron. Soc. Aust.* **4**, 53 – 55.

Subramanian, K.R., Ebenezer, E.: 2006, A statistical study of the characteristics of type II doublet radio bursts. *Astron. Astrophys.* **451**, 683 – 690. doi:10.1051/0004-6361:20054215.

Švestka, Z., Fritzová-Švestková, L.: 1974, Type II radio bursts and particle acceleration. *Solar Phys.* **36**, 417 – 431. doi:10.1007/BF00151211.

Temmer, M., Veronig, A.M., Vršnak, B., Rybák, J., *et al.*: 2008, Acceleration in fast halo CMEs and synchronized flare HXR bursts. *Astrophys. J.* **673**, L95 – L98. doi:10.1086/527414.

Thompson, B.J., Cliver, E.W., Nitta, N., Delannée, C., Delaboudinière, J.P.: 2000, Coronal dimmings and energetic CMEs in April – May 1998. *Geophys. Res. Lett.* **27**, 1431 – 1434. doi:10.1029/1999GL003668.

Thompson, B.J., Plunkett, S.P., Gurman, J.B., Newmark, J.S., St. Cyr, O.C., Michels, D.J.: 1998, SOHO/EIT observations of an Earth-directed coronal mass ejection on 12 May 1997. *Geophys. Res. Lett.* **25**, 2465 – 2468. doi:10.1029/98GL50429.

Uchida, Y.: 1968, Propagation of hydromagnetic disturbances in the solar corona and moreton's wave phenomenon. *Solar Phys.* **4**, 30 – 44. doi:10.1007/BF00146996.

Uchida, Y.: 1974, Behavior of the flare produced coronal MHD wavefront and the occurrence of type II radio bursts. *Solar Phys.* **39**, 431 – 449.

Volonskaya, N.N., Volonskaya, T.N., Semenov, V.S., Biernat, H.K.: 2003, Enargy and momentum balance in the process of time-dependent magnetic Petschek-type reconnection. *Int. J. Geomagn. Aeron.* **3**, 245 – 253.

Vršnak, B.: 2001, Solar flares and coronal shock waves. *J. Geophys. Res.* **106**, 25291 – 25300. doi:10.1029/2000JA004009.

Vršnak, B., Lulić, S.: 2000, Formation of coronal MHD shock waves – I. The basic mechanism. *Solar Phys.* **196**, 157 – 180.

Vršnak, B., Ruždjak, V., Zlobec, P., Aurass, H.: 1995, Ignition of MHD shocks associated with solar flares. *Solar Phys.* **158**, 331 – 351.

Vršnak, B., Warmuth, A., Brajša, R., Hanslmeier, A.: 2002a, Flare waves observed in Helium I 10 830 Å. A link between Hα Moreton and EIT waves. *Astron. Astrophys.* **394**, 299 – 310. doi:10.1051/0004-6361:20021121.

Vršnak, B., Magdalenić, J., Aurass, H., Mann, G.: 2002b, Band-splitting of coronal and interplanetary type II bursts. II. Coronal magnetic field and Alfvén velocity. *Astron. Astrophys.* **396**, 673 – 682. doi:10.1051/0004-6361:20021413.

Vršnak, B., Maričić, D., Stanger, A.L., Veronig, A.: 2004, Coronal mass ejection of 15 May 2001: II. Coupling of the CME acceleration and the flare energy release. *Solar Phys.* **225**, 355 – 378. doi:10.1007/s11207-004-4995-x.

Vršnak, B., Warmuth, A., Temmer, M., Veronig, A., *et al.*: 2006, Multi-wavelength study of coronal waves associated with the CME-flare event of 3 November 2003. *Astron. Astrophys.* **448**, 739 – 752. doi:10.1051/0004-6361:20053740.

Vršnak, B., Maričić, D., Stanger, A.L., Veronig, A.M., Temmer, M., Roša, D.: 2007, Acceleration phase of coronal mass ejections: I. Temporal and spatial scales. *Solar Phys.* **241**, 85 – 98. doi:10.1007/s11207-006-0290-3.

Wagner, W.J., MacQueen, R.M.: 1983, The excitation of type II radio bursts in the corona. *Astron. Astrophys.* **120**, 136 – 138.

Warmuth, A., Mann, G.: 2005, A model of the Alfvén speed in the solar corona. *Astron. Astrophys.* **435**, 1123 – 1135. doi:10.1051/0004-6361:20042169.

Warmuth, A., Mann, G., Aurass, H.: 2005, First soft X-ray observations of global coronal waves with the GOES solar X-ray imager. *Astrophys. J.* **626**, L121 – L124. doi:10.1086/431756.

Warmuth, A., Vršnak, B., Aurass, H., Hanslmeier, A.: 2001, Evolution of two EIT/Hα Moreton waves. *Astrophys. J.* **560**, L105 – L109. doi:10.1086/324055.

Warmuth, A., Vršnak, B., Magdalenić, J., Hanslmeier, A., Otruba, W.: 2004a, A multiwavelength study of solar flare waves. I. Observations and basic properties. *Astron. Astrophys.* **418**, 1101 – 1115. doi:10.1051/0004-6361:20034332.

Warmuth, A., Vršnak, B., Magdalenić, J., Hanslmeier, A., Otruba, W.: 2004b, A multiwavelength study of solar flare waves. II. Perturbation characteristics and physical interpretation. *Astron. Astrophys.* **418**, 1117 – 1129. doi:10.1051/0004-6361:20034333.

White, S.M.: 2007, Solar radio bursts and space weather. *Asian J. Phys.* **16**, 189 – 207.

White, S.M., Thompson, B.J.: 2005, High-cadence radio observations of an EIT wave. *Astrophys. J.* **620**, L63 – L66. doi:10.1086/428428.

Wild, J.P., McCready, L.L.: 1950, Observations of the spectrum of high-intensity solar radiation at metre wavelengths. I. The apparatus and spectral types of solar burst observed. *Aust. J. Sci. Res. A Phys. Sci.* **3**, 387 – 398.

Zhang, J.: 2005, A study on the acceleration of coronal mass ejections. In: Dere, K., Wang, J., Yan, Y. (eds.) *Coronal and Stellar Mass Ejections, IAU Symp.* **226**, 65–70.

Zhang, J., Dere, K.P.: 2006, A statistical study of main and residual accelerations of coronal mass ejections. *Astrophys. J.* **649**, 1100 – 1109. doi:10.1086/506903.

Zhang, J., Dere, K.P., Howard, R.A., Kundu, M.R., White, S.M.: 2001, On the temporal relationship between coronal mass ejections and flares. *Astrophys. J.* **559**, 452 – 462. doi:10.1086/322405.

Zhang, J., Dere, K.P., Howard, R.A., Vourlidas, A.: 2004, A study of the kinematic evolution of coronal mass ejections. *Astrophys. J.* **604**, 420 – 432. doi:10.1086/381725.

Zhukov, A.N., Auchère, F.: 2004, On the nature of EIT waves, EUV dimmings and their link to CMEs. *Astron. Astrophys.* **427**, 705 – 716. doi:10.1051/0004-6361:20040351.

Žic, T., Vršnak, B., Temmer, M., Jacobs, C.: 2008, Cylindrical and spherical pistons as drivers of MHD shocks. *Solar Phys.* doi:10.1007/s11207-008-9173-0. This issue.